

Towards Resiliency in Large Language Model Serving with KEVLARFLOW

Shangshu Qian¹ Kipling Liu¹ P. C. Sruthi¹ Lin Tan¹ Yongle Zhang¹

Abstract

Large Language Model (LLM) serving systems remain fundamentally fragile, where frequent hardware faults in hyperscale clusters trigger disproportionate service outages in the software stack. Current recovery mechanisms are prohibitively slow, often requiring up to 10 minutes to reinitialize resources and reload massive model weights. We introduce KEVLARFLOW, a fault tolerant serving architecture designed to bridge the gap between hardware unreliability and service availability. KEVLARFLOW leverages 1) decoupled model parallelism initialization, 2) dynamic traffic rerouting, and 3) background KV cache replication to maintain high throughput during partial failures. Our evaluation demonstrates that KEVLARFLOW reduces mean-time-to-recovery (MTTR) by 20x and, under failure conditions, improves average latency by 3.1x, 99th percentile (p99) latency by 2.8x, average time-to-first-token (TTFT) by 378.9x, and p99 TTFT by 574.6x with negligible runtime overhead in comparison to state-of-the-art LLM serving systems.

1. Introduction

LLMs have become an essential component of modern digital infrastructure, demonstrating exceptional capabilities across a wide range of tasks. However, despite their ubiquity, the infrastructure supporting LLM serving remains fundamentally fragile (Chu et al., 2025). Operational data reveals that outages are a common occurrence even for industry leaders, with significant service interruptions reported for platforms such as OpenAI (Lu, 2024) and Anthropic’s Claude (Bai, 2025). As these models are increasingly integrated into critical applications, the reliability of the underlying serving systems has emerged as a paramount concern.

¹Department of Computer Science, Purdue University, West Lafayette, IN, United States. Correspondence to: Shangshu Qian <shangshu@purdue.edu>, P. C. Sruthi <psruthi@purdue.edu>, Lin Tan <lintan@purdue.edu>, Yongle Zhang <yonglezh@purdue.edu>.

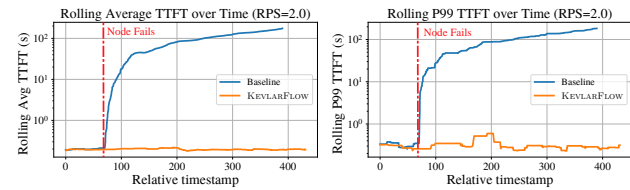


Figure 1. Rolling average and p99 TTFT comparison between a typical LLM serving framework (baseline) and KEVLARFLOW under 2 requests per second (RPS). The red line indicates the time when one node fails. Y-axis is in log scale.

The root cause of this reliability crisis is threefold. First, **hardware failures** are common in production-level GPU clusters (Cui et al., 2025; Grattafiori et al., 2024) and frequently lead to program crashes (Tiwari et al., 2015). Second, the **software stack** lacks robust fault tolerance mechanisms, further exacerbating the hardware instability. Modern LLM serving frameworks (e.g., vLLM (Kwon et al., 2023) and TensorRT-LLM (Nvidia)) rely on collective communication libraries such as Message Passing Interface (MPI) (MPI-Forum, 1994) and NVIDIA Collective Communication Library (NCCL) to implement complex model parallelism strategies (Shoeybi et al., 2019) (e.g., tensor and pipeline parallelism). Such communication libraries often optimize for throughput instead of fault tolerance (Hu et al., 2025; Wengram et al., 2023) and create complex inter-dependencies among participating nodes since the initialization of the serving program. As a result, the failure of a single node will render all other model parallelism participants, while still alive, unserviceable for user requests. Figure 1 (blue lines) shows the rolling average and p99 TTFT of a typical LLM serving cluster under node failures. When one node fails, incoming requests pile up the queue quickly due to reduced serving capacity, increasing the TTFT and affecting user experience.

Third, **slow recovery** of LLM serving systems compounds these software and hardware issues by prolonging service degradation after a failure. Restoring a failed instance typically involves 1) a complete re-initialization of serving node (e.g., one instance on Amazon EC2), and 2) the reloading of massive model weights from remote storage. This process can take as long as 10 minutes (Jaiswal et al., 2025b), and the LLM service (partially) backed by the failed node will remain *unresponsive* during the entire recovery time.

Furthermore, widely used redundancy techniques from traditional distributed systems, such as data replication, have not been seamlessly adapted for the memory-intensive and state-heavy nature of LLM inference (Strati et al., 2024). While replication ensures high availability in databases, applying it to LLM serving remaining a challenging problem due to the unique constraints of GPU memory and the transient nature of the inference state.

To address these challenges, we introduce KEVLARFLOW, a fault tolerant serving architecture designed to bridge the gap between hardware unreliability and service availability. To solve the hardware instability, KEVLARFLOW draws insight from the inherent redundancy found within the load balancer groups of serving systems (Jain et al., 2025). By treating the cluster not as a collection of rigid, independent instances but as a flexible pool of resources, KEVLARFLOW enables high-throughput serving that degrades gracefully rather than failing catastrophically.

KEVLARFLOW achieves resiliency in LLM serving through three novel design contributions:

1. Dynamic Traffic Rerouting and Partial Availability.

KEVLARFLOW introduces a traffic management strategy that handles partial model parallelism failures – scenarios where only a subset of nodes in a model parallel group fails. Instead of marking the entire instance as offline, KEVLARFLOW dynamically reroutes user traffic around the failed node to other healthy instances in the load balancing group. Crucially, it keeps the remaining healthy parts of the damaged model in service, allowing failed nodes to be replaced in the background. This approach significantly improves system throughput under failure conditions by preventing the waste of functional GPU resources blocked by dependencies.

2. Decoupled Model Parallelism Initialization.

Unlike other frameworks, KEVLARFLOW decouples the initialization of model parallelism communicator from model weight loading, instead of performing both tasks at the start of the service. This architectural separation allows for dynamic reconfigurations of the parallelism schemes at runtime. If a node fails, the system can re-establish communication among the remaining healthy nodes without incurring the heavy overhead of a full restart or weight reload.

3. Background KV Cache Replication.

To mitigate the latency penalty of request restarting, KEVLARFLOW implements a low-overhead background replication mechanism for the KV cache. By replicating the intermediate inference state to other nodes in the load balancing group during runtime, KEVLARFLOW ensures that if a failure occurs, partially served requests can be continued near-instantly on a live node. This replication converts what would be a hard failure requiring a restart into a seamless migration, preserving the user’s session context.

Our evaluation demonstrates that KEVLARFLOW effectively masks hardware failures with minimal performance penalties:

1. Under partial failure scenarios, KEVLARFLOW improves average latency by 3.1x, p99 latency by 2.8x, average TTFT by 378.9x, and p99 TTFT by 574.6x compared to failure behaviors in state-of-the-art LLM serving frameworks.
2. KEVLARFLOW shortens the mean-time-to-recovery (MTTR) of node failures from 10 minutes (Jaiswal et al., 2025b) to 30 seconds, a 20x improvement.
3. The background KV cache replication incurs negligible overhead during normal operations, highlighting KEVLARFLOW’s potential as an “always-on” fault tolerance solution for the next-generation AI infrastructure.

KEVLARFLOW is the first LLM serving framework that can tolerate runtime node failures, allowing non-interruptive request handling during failure recovery.

2. Related Work

In this section, we introduce existing fault tolerance mechanisms in both LLM training and serving applications, and show that KEVLARFLOW is the only approach that can tolerate node failures in serving applications.

Fault-Tolerant LLM Training.

Communication and computation patterns are fundamentally different in LLM training and serving applications. Fault tolerance training techniques (Gandhi et al., 2024; Duan et al., 2024) do not directly apply to serving for two reasons: 1) serving maintains transient states (i.e., KV cache) for each request between multiple forward passes, while training computes the model output in a single forward pass, and 2) serving has stricter latency requirements (e.g., TTFT) beyond throughput.

Existing checkpoint or migration based fault tolerance mechanisms (Wang et al., 2023; Jiang et al., 2024) in training cannot be directly applied in serving due to the lack of ability to capture KV cache. Moreover, even with checkpoints, ongoing requests are still paused during failure recovery, which exacerbates latency requirements potentially leading to SLO violations. Pipeline adaptation methods such as ReCycle (Gandhi et al., 2024) rely on redirecting work into schedule bubbles. However, since LLM serving performs only a forward pass, it lacks the exploitable bubbles found in training schedules, rendering such techniques ineffective for inference fault tolerance.

Fault-Tolerant LLM Serving.

Fault tolerance in LLM serving has evolved in two stages. The first is KV cache preservation through migration. DejaVu (Strati et al., 2024)

streams KV cache to CPU or remote memory for fast recovery, whereas SpotServe (Miao et al., 2024) migrates state during preemption grace periods (~ 30 s). However, both approaches require restarting the serving instance after topology changes (i.e., recreating communicators and reloading state) which hurts latency and TTFT.

Recent efforts in this area focus on fault-tolerant communicators. AnchorTP (Xu et al., 2025) preserves inference states via daemons for elastic tensor parallelism, but only tolerates intra-node GPU failures and requires weight migration between GPUs with KV cache recomputation, which adds latency. R²CCL (Wang et al., 2025a) provides NIC failover by utilizing multi-NIC hardware, but only tolerates NIC failures instead of node failures. Both mechanisms share a fundamental limitation. They treat the LLM serving instance as *a single fault domain*, and cannot tolerate the failure of the serving node itself.

In contrast, KEVLARFLOW splits each LLM serving instance into multiple fault domains (i.e., independent nodes), and achieves continuous request handling after node failures through decoupled initialization, which enables re-establishing serving instances with existing healthy nodes in the load balancing group, maximizing the resource utilization, and minimizing the service downtime needed for either reloading/migrating model weights or re-provisioning additional resources in existing approaches.

Other LLM serving systems focus on efficiency rather than fault tolerance. Dynamic scheduling approaches (Wu et al., 2024; Fu et al., 2024; Sun et al., 2024) and prefill-decode disaggregation (Zhong et al., 2024; Agrawal et al., 2024) optimize resource utilization and latency but do not focus on fault tolerance.

3. Design of KEVLARFLOW

Current LLM serving infrastructure suffers from a mismatch between the stochastic nature of hardware and the immutability assumptions in the software stack. While GPU clusters face high-frequency component failures (Grattafiori et al., 2024), software abstractions typically treat the cluster as immutable. KEVLARFLOW addresses this by abandoning the traditional “fail-stop” paradigm for a “fail-stutter” fault tolerance model (Arpaci-Dusseau & Arpaci-Dusseau, 2001). Using novel mechanisms of 1) decoupled initialization, 2) dynamic traffic rerouting, and 3) continuous state replication (Section 3.2), KEVLARFLOW decouples logical availability from physical node health, transforming LLM serving infrastructures into a self-healing fabric.

3.1. Background and Motivation

LLM serving systems generally employ a controller-worker architecture, comprising a centralized request metadata handler and multiple model executors. These executors are mapped to *ranks* in a communication group (i.e., communicator) managed by libraries such as MPI or NCCL. In model parallelism deployments, the metadata handler often resides on the first rank. The initialization process of these serving instances generally follows a three-step sequence:

1. A **state sharing mechanism** is established to facilitate metadata exchange. This is commonly implemented via a PyTorch store (e.g., TCPStore in `torch.distributed`) (Li et al., 2020) or more sophisticated ones with MPI.
2. The system configures the **collective communicator** (e.g., an NCCL communicator) using the state sharing mechanism to define the topology for inter-device communications (e.g., `allreduce` operations).
3. The **model weights** are loaded, and the inference logic is configured to execute according to the model parallelism scheme (Li et al., 2020).

While effective for performance, this architecture suffers from significant drawbacks regarding fault tolerance:

1. **Static Device Topology:** The device topology and communicator scope are fixed at startup (Wang et al., 2025a). For instance, `MPI_COMM_WORLD` is defined upon program launch and is immutable (Schulz, 2023). Adding or removing ranks from an existing communicator to handle failures or scaling is not fully supported (mixen56, 2025), often necessitating a full system restart instead.
2. **Risks of Tensor Parallelism:** While intra-node tensor parallelism minimizes latency and maximizes throughput (Narayanan et al., 2021; Shoeybi et al., 2019), it introduces a *single point of failure*: the node itself. A failure in power or network connectivity for the node brings down the entire tensor parallel group. Additionally, the reliance on proprietary high-bandwidth interconnects (e.g., NVLink and NVSwitch) enforces vendor lock-in and restricts accessibility for academic and smaller entities (Hooker, 2021).

3.2. The KEVLARFLOW Solution

To address the drawbacks of existing systems, KEVLARFLOW adopts two core design principles: 1) reduce single points of failure, and 2) minimize data and control dependencies between model parallel ranks.

KEVLARFLOW leverages the existing redundancy of model weights in load balancing groups, where multiple replicas of the model are used to handle concurrent user traffic (Jain et al., 2025). We adopt the multi-node pipeline parallelism as our base model parallelism scheme, which has gained

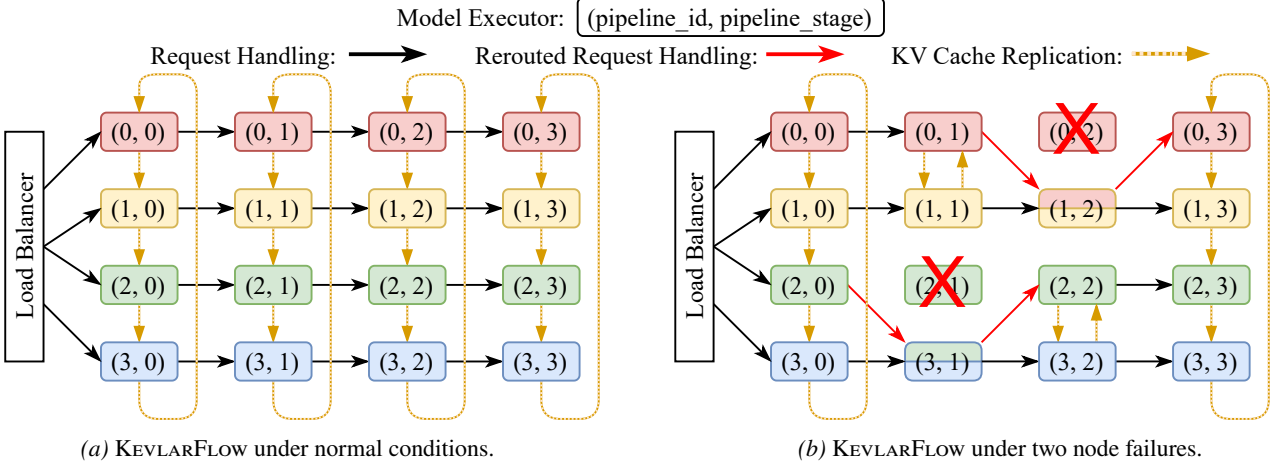


Figure 2. Design of KEVLARFLOW. The example shows a 4-stage pipeline parallelism serving (i.e., the model weights are split to four model executors). The load balancing group has four active model instances. A red “X” indicate a failed node.

significant traction in recent years (Zhang et al., 2025b; JIANG et al., 2025; Guo et al., 2025; Lin et al., 2025; Luo et al., 2025; Ma et al., 2024) due to its distinct advantages over tensor parallelism: it 1) creates multiple independent fault domains for isolation, 2) achieves high throughput with low bandwidth requirements, and 3) eliminates the need for specialized interconnect hardware.

As illustrated in Figure 2, KEVLARFLOW enhances this baseline architecture with three novel components to ensure fault tolerance properties:

1. Decoupled Model Parallelism Initialization. We redesign the initialization process of LLM serving with a ground-up approach. Instead of relying on a single master process to coordinate a static global state, we use a decoupled model parallelism initialization process, where participating nodes autonomously connect to one another. The communication communicator is constructed only after nodes have been connected and verified as healthy.

This decoupling enables dynamic reconfiguration of the device topology. In the event of a node failure, the surviving nodes can rapidly identify a replacement node within the fault tolerance group and establish a new serving pipeline without tearing down the entire cluster. Figure 2b shows an example of this process. When node (0, 2) fails, node (0, 1) and (0, 3) quickly identifies another healthy node (1, 2), which holds the same portion of model weights as node (0, 2), to replace it. A new communicator and serving pipeline is formed promptly once the node failure is detected (more details below).

2. Dynamic Traffic Rerouting. Enabled by the decoupled initialization, KEVLARFLOW uses dynamic traffic rerouting when one pipeline is only partially available. In existing frameworks, a single node failure (e.g., node (0, 2) in

Figure 2b) interrupts the entire communicator, rendering all associated healthy GPUs (e.g., node (0, 0), (0, 1), and (0, 3)) idle and causing a total loss of that instance’s serving capacity.

On the contrary, KEVLARFLOW contains the failure locally. When a node failure happens, KEVLARFLOW dynamically reroutes user traffic around the failed node (i.e., red arrows in Figure 2b) through the newly created communicator. This ensures that the capacity drop is limited strictly to the failed node, while all other healthy nodes continue to process requests.

3. Background KV Cache Replication. Current LLM serving systems utilize a KV cache to accelerate inference by storing attention states. Such data is usually stored in GPU memory or swapped to CPU memory under CUDA unified memory (NVidia, 2025), and will be lost once the node failure happens, forcing a retry of the entire request.

To enable non-interruptive service, KEVLARFLOW replicates KV cache for each request to the GPU memory of other nodes in the load balancing group (e.g., yellow arrows in Figure 2a). When failure occurs, a new serving pipeline involving the replication target (e.g., node (1, 2)) is established. In-progress requests will be served continuously on the replication target from the replicated state, avoiding retries and significantly reducing tail latency under failure conditions.

When node failure happens and the system is in a degraded state, KV cache replication targets will be automatically adjusted to exclude the nodes under traffic rerouting. For example, nodes (0, 2), (1, 2), (2, 1), and (3, 1) in Figure 2b are excluded from KV cache replication. And the replication targets of nodes (1, 1) and (3, 2) are adjusted to other healthy nodes.

To avoid interference with request handling, KEVLARFLOW uses a block representation of KV cache (Kwon et al., 2023) and replicate it block-by-block in the background. A separate CUDA stream is used to overlap the communication with computation.

A common concern is whether sufficient GPU memory exists to handle both the rerouted traffic and replication KV cache. Analyses of production workload traces (Patke et al., 2025; Huang et al., 2024; Jaiswal et al., 2025a; Zhang et al., 2025a) show that GPU is rarely saturated during serving, often fluctuating around 50% - 60% utilization to preserve memory headroom to ensure service level objectives (SLOs).

KEVLARFLOW utilizes such memory headroom to temporarily handle rerouted traffic and the replicated KV cache. When memory pressure happens, KEVLARFLOW drops the replicated KV cache and recomputes them if needed.

3.3. Implementation Details

KEVLARFLOW is implemented on top of TensorRT-LLM’s PyTorch backend (Nvidia), a high performance LLM serving framework, providing an OpenAI-compatible server endpoint. Each node has a gRPC-based (Google) RPC endpoint to facilitate inter-node communication (e.g., the formation of pipeline communicator).

We port TensorRT-LLM to MPICH (Gropp & Lusk, 1996) instead of using its original dependency of OpenMPI (Gabriel et al., 2004) due to MPICH’s robust implementation of MPI_Open_port, MPI_Comm_connect, and MPI_Intercomm_merge functionalities. All are crucial for KEVLARFLOW’s implementation of decoupled model parallelism initialization and traffic rerouting.

KEVLARFLOW use NCCL to implement KV cache replication, enabling direct GPU-to-GPU replication when GPUDirect RDMA links are available. A distributed lock (Hastings, 1990) is implemented with PyTorch’s TCPStore (Li et al., 2020) to avoid deadlocks in the ring-shaped KV cache replication scheme (Figure 2a) due to limitations in the NCCL’s send and recv functions.

4. Evaluation

We evaluate KEVLARFLOW using two virtual clusters rented from industry-leading cloud providers. One cluster is equipped with eight server nodes, and the other with 16 nodes. Each node has one NVIDIA A10 Tensor Core GPU with 24GB GDDR6 memory. Nodes within each cluster are distributed across four different datacenter locations in the eastern, central, western, and southern parts of the United States, simulating a geo-distributed load balancing group.

Each node is connected to Internet through a 1Gbps Ethernet port, and does not have any specialized interconnection

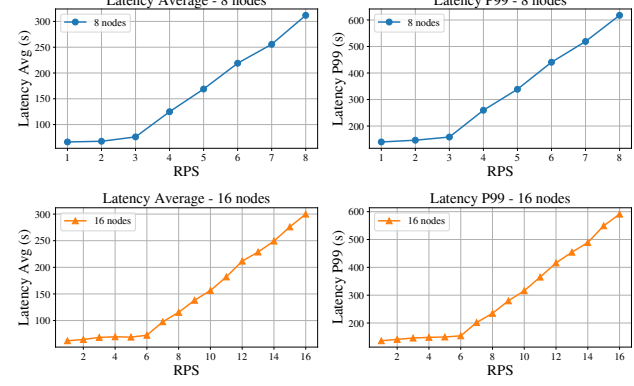


Figure 3. Baseline latency performance of TensorRT-LLM. The performance of 8-node cluster is marked with blue dots, and that of the 16-node cluster is marked with orange triangles. Figures on the left are for the average latency, and figures on the right are for the p99 latency.

hardware (e.g., InfiniBand). Nodes in different datacenters are in different autonomous systems (AS), connected through commercial Internet transit providers (e.g., Areion, Level 3, and GTT), simulating *affordable* computing resources available to academic research groups.

We simulate requests to LLM serving systems using requests from ShareGPT (ShareGPT), a popular (Gao et al., 2025; Fu et al., 2024; Wang et al., 2025b; Xiang et al., 2025; Song et al., 2026; Gong et al., 2025; Zhao & Wang, 2024; He et al., 2025; Wu et al., 2024; Patke et al., 2024; Papaioannou & Doudali, 2024; Zhong et al., 2024; Feng et al., 2025) dataset evaluating the performance of LLM serving systems. We simulate the arrival time of requests using Poisson distribution under different parameters of request rate (RPS, or request per second).

We use Llama-3.1-8B model (Meta, 2024) with a 4-stage pipeline parallelism on our serving instances. Each pipeline stage is served on one node in the virtual cluster. We place each model instance on four nodes located in the same datacenter. In the first virtual cluster with eight nodes, the load balancing group has two model instances. In the second virtual cluster with 16 nodes, the load balancing group has four model instances. The load balancer distributes requests evenly across all instances in the load balancing group.

To evaluate KEVLARFLOW’s performance, we focus on answering the following questions:

1. How does KEVLARFLOW perform under node failures?
2. How much improvement does KEVLARFLOW have on failure recovery time?
3. How much overhead does KEVLARFLOW introduce?

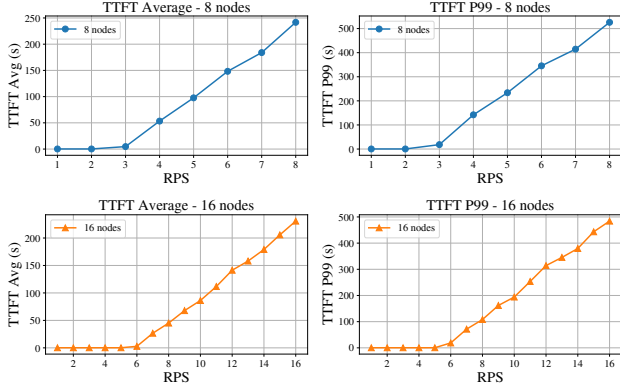


Figure 4. Baseline TTFT of TensorRT-LLM. The performance of 8-node cluster is marked with blue dots, and that of the 16-node cluster is marked with orange triangles. Figures on the left are for the average TTFT, and figures on the right are for the p99 TTFT.

4.1. Baseline Performance

We first establish the baseline performance of TensorRT-LLM on our virtual clusters. Figure 3 shows the baseline latency of TensorRT-LLM serving Llama-3.1-8B with a 4-stage pipeline parallelism. The figure shows both the average and p99 latency on the 8-node and 16-node cluster. In the 8-node cluster, request latency starts to grow when the RPS (request/sec) increases from 3 to 4, indicating a significant growth request queue. Similar transition exists in the 16-node cluster when RPS grows from 6 to 7. This is expected as the 16-node cluster doubles the capacity of the 8-node cluster.

Time-to-first-token (TTFT), an important measurement for the service level objectives (SLOs) (Hong et al., 2025), shows a similar trend as the latency. As shown in Figure 4, requests start to queue up at a RPS of 3 in the 8-node cluster and at a RPS of 6 in the 16-node cluster.

Time-per-output-token (TPOT), a metric measuring the per-token latency of LLM serving instances, remains nearly constant in all baseline benchmark scenarios, with an average TPOT of 163ms/token and a p99 TPOT of 203ms/token. This is the behavior of TensorRT-LLM’s default batch scheduler, and we use it in all our benchmark to ensure a fair comparison.

4.2. Performance Under Node Failure

To demonstrate KEVLARFLOW’s fault tolerance capabilities, we evaluate KEVLARFLOW under node failures against the standard fault behavior (Section 1, Section 3.2): when one node in the serving pipeline fails, the entire pipeline ceases to serve user requests. Under standard fault behavior, the load balancer will distribute incoming requests evenly to the remaining healthy pipelines. Any in-progress requests will be immediately retried once the node failure is detected.

Generality of the standard fault behavior. As discussed in Section 1 and Section 3.1, existing collective communication libraries such as MPI and NCCL assume a static device topology, and state-of-the-art serving frameworks (e.g., TensorRT-LLM, vLLM) strictly adhere to this assumption. KEVLARFLOW distinguishes itself as the first LLM serving framework capable of tolerating runtime node failures without service interruption. In contrast, all existing fault-tolerant approaches, including DejaVu (Strati et al., 2024), AnchorTP (Xu et al., 2025), and R²CCL (Wang et al., 2025a), would follow the standard fault behavior. Thus, the comparative evaluation presented in this section is applicable to all such systems.

We compare KEVLARFLOW against standard fault behavior under three scenarios:

1. In the 8-node cluster, we inject failure to one node, failing one pipeline in the load balancing group.
2. In the 16-node cluster, we inject failure to one node, failing one pipeline in the load balancing group.
3. In the 16-node cluster, we inject failures to two nodes, failing two pipelines in the load balancing group.

Figure 5 shows the comparison of average latency, average TTFT, p99 latency, and p99 TTFT of KEVLARFLOW against the standard fault behavior under three different fault scenarios. KEVLARFLOW achieves an improvement in average latency, p99 latency, average TTFT, and p99 TTFT of up to **3.1x**, **2.8x**, **378.9x**, and **574.6x** respectively. Detailed data of the benchmark can be found in Table 1 in the appendix.

Explanation of the massive TTFT improvement. In the event of a node failure, KEVLARFLOW utilizes dynamic traffic rerouting to keep the remaining healthy nodes of the degraded pipeline operational. This approach preserves a significantly larger fraction of the load balancing group’s capacity compared to standard fault behavior, which often render an entire pipeline unusable upon a single failure. Consequently, KEVLARFLOW delays system saturation, allowing the scheduler to handle higher request rates without accumulating a backlog of queued requests.

Figure 6 illustrates the rolling average and p99 TTFT for failure scenario 1 at an RPS of 2.0, where KEVLARFLOW demonstrates its most substantial improvement over the baseline. Upon node failure, serving clusters operating under standard fault behavior rapidly accumulate a backlog of queued requests, causing immediate spikes in the TTFT of incoming traffic. In contrast, KEVLARFLOW leverages dynamic traffic rerouting and KV cache replication to sustain uninterrupted request handling, thereby maintaining stable average and p99 TTFT. As shown in Figure 7, this resilience persists even when the serving system is saturated (i.e., RPS > 3 in scenario 1, and RPS ≥ 6 in scenarios 2 and 3).

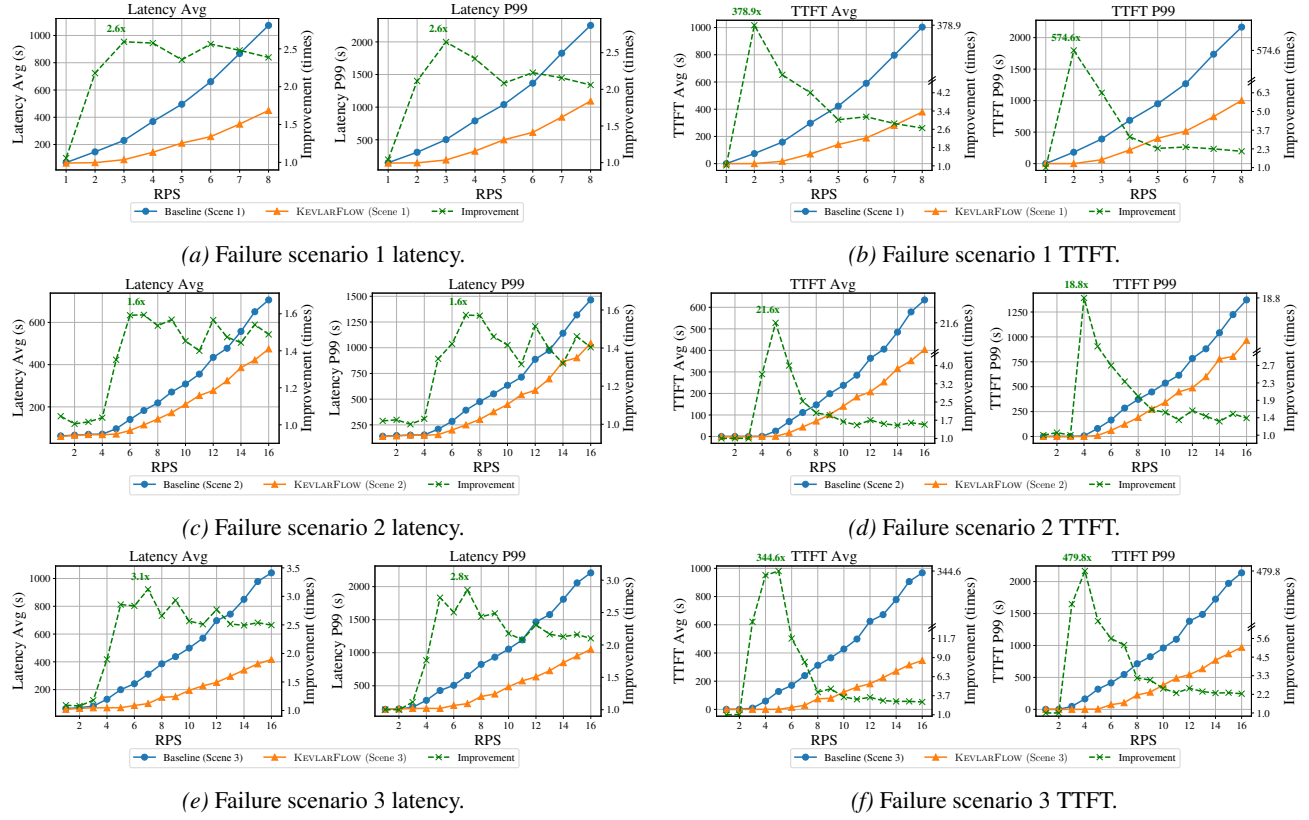


Figure 5. Comparison of KEVLARFLOW and baseline under three node failure scenarios. Performance of the standard fault behavior is plotted using blue dots, KEVLARFLOW’s performance is plotted in orange triangles. The improvement of KEVLARFLOW over the standard fault behavior is plotted in green dotted lines. The highest improvement is annotated in each figure.

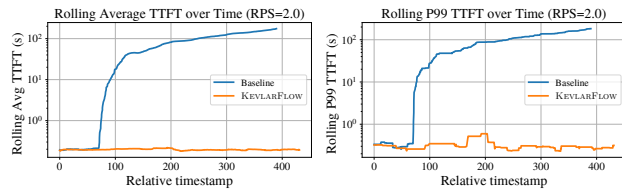


Figure 6. Rolling average and p99 TTFT over time under node failure scenario 1 (RPS=2.0). KEVLARFLOW is represented by the orange line, and standard fault behavior is represented by the blue line. Y-axis is in log scale.

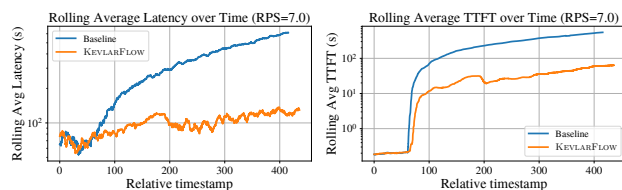


Figure 7. Rolling average latency and TTFT over time under node failure scenario 3 (RPS=7.0). KEVLARFLOW is represented by the orange line, and standard fault behavior is represented by the blue line. Y-axis is in log scale.

KEVLARFLOW delivers significant performance gains over standard fault behavior – achieving improvements of up to 3.18x, 2.71x, and 5.64x in scenarios 1, 2, and 3, respectively – underscoring the versatility of KEVLARFLOW under diverse load conditions.

4.3. Failure Recovery Time

Current LLM serving systems suffer from prolonged error recovery times due to the heavy overhead of instance initialization and model weight loading. This process can take up to 10 minutes (Jaiswal et al., 2025b). During this downtime, the serving instance remains completely unresponsive to user requests. Standard KV cache replication techniques, such as DejaVu (Strati et al., 2024), are ineffective at accelerating this specific recovery phase because they rely on the existence of a live serving instance to receive the state, which is unavailable during a hard node failure.

KEVLARFLOW addresses this by leveraging decoupled initialization and dynamic traffic rerouting to enable rapid service restoration. Upon detecting a node failure, KEVLARFLOW automatically: 1) locates a healthy alternative node within the load balancing group that holds the same model

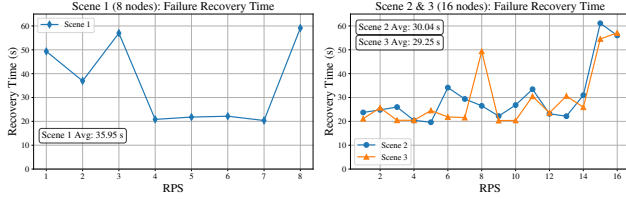


Figure 8. Failure recovery time of KEVLARFLOW under three failure scenarios.

weights, 2) re-establishes the inter-node communicator, and 3) resumes the processing of user requests. This recovery mechanism overlaps the lengthy full-instance initialization with a degraded yet functional serving pipeline, significantly reducing both latency and TTFT for user requests during failure events.

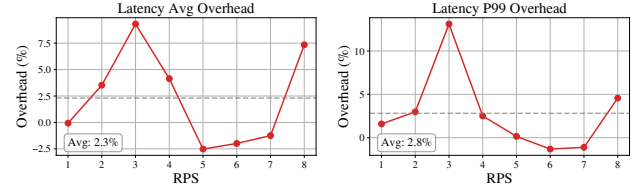
Figure 8 illustrates the failure recovery time of KEVLARFLOW across the three scenarios defined in Section 4.2. KEVLARFLOW achieves an average recovery time of 35s in scenario 1, 30s in scenario 2, and 29s in scenario 3. These results represent a **20x** improvement over the mean-time-to-recovery (MTTR) of state-of-the-art LLM serving systems.

Note that user requests continue to be processed throughout KEVLARFLOW’s failure recovery phase. As shown in Figure 8, the recovery duration does not increase with the RPS. Instead, it fluctuates marginally around the average value. This stability demonstrates KEVLARFLOW’s scalability and its ability to maintain consistent fault tolerance under varying workload intensities.

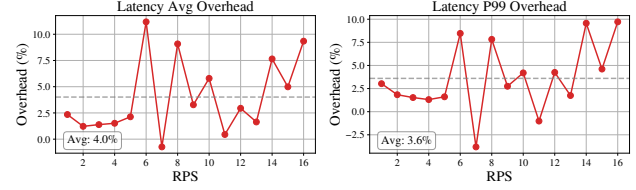
Comparison with hot spare approaches. Another strategy for reducing failure recovery time is leveraging hot spare nodes (Miao et al., 2024), which remain online but idle during normal operations. While this allows for rapid replacement upon node failure, it inherently wastes valuable GPU resources. In contrast, KEVLARFLOW employs dynamic traffic rerouting to maintain continuous service using all available healthy nodes, while replacement resources are initialized in the background. Consequently, KEVLARFLOW offers superior cost-efficiency compared to hot spare approaches, as it eliminates the need to provision redundant, idle GPU capacity at system startup.

4.4. Runtime Overhead

A critical requirement for fault-tolerant serving systems is minimizing the performance penalty imposed during normal, failure-free operation. We evaluate the overhead of KEVLARFLOW by measuring the impact of its continuous background KV cache replication on end-to-end serving latency.



(a) Overhead in the 8-node cluster.



(b) Overhead in the 16-node cluster.

Figure 9. Runtime overhead of KEVLARFLOW. Some overhead values are negative due to non-determinism in the execution. We consider them as 0% overhead in practice.

As detailed in Section 3.2, KEVLARFLOW mitigates resource contention by performing block-wise KV cache replication on a dedicated CUDA stream, effectively overlapping communication costs with computation.

Our evaluation confirms that KEVLARFLOW incurs **minimal runtime overhead** compared to the baseline. As shown in Figure 9a, the 8-node cluster exhibits an average latency overhead of only 2.3% and a p99 overhead of 2.8%. Similarly, Figure 9b shows that on the larger 16-node cluster, the average and p99 overheads remain constrained to 4.0% and 3.6%, respectively. The overhead fluctuates across different RPS rates while occasionally dropping below zero due to non-determinism in execution. It confirms that the background replication does not introduce systematic contention. This low overhead highlights KEVLARFLOW’s viability as an “always-on” fault tolerance solution for the hyper-scale AI infrastructure.

5. Conclusion

We present KEVLARFLOW, a fault tolerant LLM serving architecture that bridges the gap between unreliable hardware and reliable LLM services. Our extensive evaluation on geo-distributed clusters demonstrates that KEVLARFLOW significantly enhances LLM serving systems’ fault tolerant properties. It reduces the MTTR by **20x** – from 10 minutes to roughly 30 seconds. Furthermore, under partial failure conditions, KEVLARFLOW improves average and p99 TTFT by up to **378.9x** and **574.6x** respectively in comparison to state-of-the-art LLM serving systems with negligible runtime overhead during normal operations.

Acknowledgments

The authors thank David Helsel for helping with the implementations. This research is partially supported by NSF 1901242, 2006688, 2300562, and a Meta Research Award. Any opinions, findings, and conclusions in this paper are those of the authors only and do not necessarily reflect the views of the sponsors.

Impact Statement

This paper presents work whose goal is to advance the field of Machine Learning. There are many potential societal consequences of our work, none which we feel must be specifically highlighted here.

References

Agrawal, A., Kedia, N., Panwar, A., Mohan, J., Kwatra, N., Gulavani, B. S., Tumanov, A., and Ramjee, R. Taming throughput-latency tradeoff in LLM inference with sarathi-serve. In *Proceedings of the 18th USENIX Conference on Operating Systems Design and Implementation*, OSDI’24, pp. 117–134, USA, July 2024. USENIX Association. ISBN 978-1-939133-40-3.

Arpaci-Dusseau, R. H. and Arpaci-Dusseau, A. C. Fail-stutter fault tolerance. In *Proceedings Eighth Workshop on Hot Topics in Operating Systems*, pp. 33–38. IEEE, 2001.

Bai, Y. Understanding service reliability of large language models: An empirical characterization on operator and user reports. Master’s thesis, Universiteit van Amsterdam, 2025. Available at <https://atlarge-research.com/pdfs/2025-msc-ybai.pdf>.

Chu, X., Talluri, S., Lu, Q., and Iosup, A. An empirical characterization of outages and incidents in public services for large language models. In *Proceedings of the 16th ACM/SPEC International Conference on Performance Engineering*, pp. 69–80, 2025.

Cui, S., Patke, A., Nguyen, H., Ranjan, A., Chen, Z., Cao, P., Bauer, G., Bode, B., Martino, C. D., Jha, S., et al. Story of two gpus: Characterizing the resilience of hopper h100 and ampere a100 gpus. In *Proceedings of the International Conference for High Performance Computing, Networking, Storage and Analysis*, pp. 1145–1164, 2025.

Duan, J., Song, Z., Miao, X., Xi, X., Lin, D., Xu, H., Zhang, M., and Jia, Z. Parcae: Proactive, liveput-optimized DNN training on preemptible instances. In *Proceedings of the 21st USENIX Symposium on Networked Systems Design and Implementation*, NSDI’24, pp. 1121–1139, USA, April 2024. USENIX Association. ISBN 978-1-939133-39-7.

Feng, J., Huang, Y., Zhang, R., Liang, S., Yan, M., and Wu, J. Windserve: Efficient phase-disaggregated llm serving with stream-based dynamic scheduling. In *Proceedings of the 52nd Annual International Symposium on Computer Architecture*, pp. 1283–1295, 2025.

Fu, Y., Xue, L., Huang, Y., Brabete, A.-O., Ustiugov, D., Patel, Y., and Mai, L. *serverlessllm:low – latency* serverless inference for large language models. In *18th USENIX Symposium on Operating Systems Design and Implementation (OSDI 24)*, pp. 135–153, 2024.

Gabriel, E., Fagg, G. E., Bosilca, G., Angskun, T., Dongarra, J. J., Squyres, J. M., Sahay, V., Kambadur, P., Barrett, B., Lumsdaine, A., et al. Open mpi: Goals, concept, and design of a next generation mpi implementation. In *European Parallel Virtual Machine/Message Passing Interface Users’ Group Meeting*, pp. 97–104. Springer, 2004.

Gandhi, S., Zhao, M., Skiadopoulos, A., and Kozyrakis, C. ReCycle: Resilient Training of Large DNNs using Pipeline Adaptation. In *Proceedings of the ACM SIGOPS 30th Symposium on Operating Systems Principles*, SOSP ’24, pp. 211–228, New York, NY, USA, November 2024. Association for Computing Machinery. ISBN 979-8-4007-1251-7. doi: 10.1145/3694715.3695960. URL <https://dl.acm.org/doi/10.1145/3694715.3695960>.

Gao, S., Zhang, X., Shen, Y., and Chen, L. Apt-serve: Adaptive request scheduling on hybrid cache for scalable llm inference serving. *Proceedings of the ACM on Management of Data*, 3(3):1–28, 2025.

Gong, R., Bai, S., Wu, S., Fan, Y., Wang, Z., Li, X., Yang, H., and Liu, X. Past-future scheduler for llm serving under sla guarantees. In *Proceedings of the 30th ACM International Conference on Architectural Support for Programming Languages and Operating Systems*, Volume 2, pp. 798–813, 2025.

Google. gRPC. <https://grpc.io/>.

Grattafiori, A., Dubey, A., Jauhri, A., Pandey, A., Kadian, A., Al-Dahle, A., Letman, A., Mathur, A., Schelten, A., Vaughan, A., et al. The llama 3 herd of models. *arXiv preprint arXiv:2407.21783*, 2024.

Gropp, W. and Lusk, E. User’s guide for mpich, a portable implementation of mpi, 1996.

Guo, T., Zhang, X., Du, J., Chen, Z., Xiao, N., and Lu, Y. gllm: Global balanced pipeline parallelism systems for distributed llms serving with token throttling. In *Proceedings of the International Conference for High Performance Computing, Networking, Storage and Analysis*, pp. 1725–1741, 2025.

Hastings, A. B. Distributed lock management in a transaction processing environment. In *Proceedings Ninth Symposium on Reliable Distributed Systems*, pp. 22–31. IEEE, 1990.

He, Y., Yang, H., Lu, Y., Klimovic, A., and Alonso, G. Resource multiplexing in tuning and serving large language models. In *2025 USENIX Annual Technical Conference (USENIX ATC 25)*, pp. 1639–1655, 2025.

Hong, K., Li, X., Chen, L., Mao, Q., Dai, G., Ning, X., Yan, S., Liang, Y., and Wang, Y. Sola: Optimizing slo attainment for large language model serving with state-aware scheduling. *Proceedings of Machine Learning and Systems*, 7, 2025.

Hooker, S. The hardware lottery. *Communications of the ACM*, 64(12):58–65, 2021.

Hu, Z., Shen, S., Bonato, T., Jeaugey, S., Alexander, C., Spada, E., Dinan, J., Hammond, J., and Hoefer, T. Demystifying nccl: An in-depth analysis of gpu communication protocols and algorithms. In *2025 IEEE Symposium on High-Performance Interconnects (HOTI)*, pp. 48–59. IEEE, 2025.

Huang, T., Chen, P., Gong, K., Hawk, J., Bright, Z., Xie, W., Huang, K., and Ji, Z. Enova: Autoscaling towards cost-effective and stable serverless llm serving. *arXiv preprint arXiv:2407.09486*, 2024.

Jain, K., Parayil, A., Mallick, A., Choukse, E., Qin, X., Zhang, J., Goiri, I., Wang, R., Bansal, C., Rühle, V., et al. Performance aware llm load balancer for mixed workloads. In *Proceedings of the 5th Workshop on Machine Learning and Systems*, pp. 19–30, 2025.

Jaiswal, S., Jain, K., Simmhan, Y., Parayil, A., Mallick, A., Wang, R., Amant, R. S., Bansal, C., Rühle, V., Kulkarni, A., et al. Sageserve: Optimizing llm serving on cloud data centers with forecast aware auto-scaling. *Proceedings of the ACM on Measurement and Analysis of Computing Systems*, 9(3):1–24, 2025a.

Jaiswal, S., Jain, K., Simmhan, Y., Parayil, A., Mallick, A., Wang, R., Amant, R. S., Bansal, C., Rühle, V., Kulkarni, A., et al. Serving models, fast and slow: optimizing heterogeneous llm inferencing workloads at scale. *arXiv preprint arXiv:2502.14617*, 2025b.

JIANG, Y., Fu, F., Yao, X., Wang, T., CUI, B., Klimovic, A., and Yoneki, E. Thunderserve: High-performance and cost-efficient LLM serving in cloud environments. In *Eighth Conference on Machine Learning and Systems*, 2025. URL <https://openreview.net/forum?id=44PwmgOpAt>.

Jiang, Z., Lin, H., Zhong, Y., Huang, Q., Chen, Y., Zhang, Z., Peng, Y., Li, X., Xie, C., Nong, S., Jia, Y., He, S., Chen, H., Bai, Z., Hou, Q., Yan, S., Zhou, D., Sheng, Y., Jiang, Z., Xu, H., Wei, H., Zhang, Z., Nie, P., Zou, L., Zhao, S., Xiang, L., Liu, Z., Li, Z., Jia, X., Ye, J., Jin, X., and Liu, X. MegaScale: Scaling large language model training to more than 10,000 GPUs. In *Proceedings of the 21st USENIX Symposium on Networked Systems Design and Implementation, NSDI’24*, pp. 745–760, USA, April 2024. USENIX Association. ISBN 978-1-939133-39-7.

Kwon, W., Li, Z., Zhuang, S., Sheng, Y., Zheng, L., Yu, C. H., Gonzalez, J., Zhang, H., and Stoica, I. Efficient memory management for large language model serving with pagedattention. In *Proceedings of the 29th symposium on operating systems principles*, pp. 611–626, 2023.

Li, S., Zhao, Y., Varma, R., Salpekar, O., Noordhuis, P., Li, T., Paszke, A., Smith, J., Vaughan, B., Damania, P., et al. Pytorch distributed: experiences on accelerating data parallel training. *Proceedings of the VLDB Endowment*, 13(12):3005–3018, 2020.

Lin, Y., Peng, S., Wu, S., Li, Y., Lu, C., Ye, K., and Xu, C. Serving llm in distributed gpu cluster with fine-grain pipeline constraints. *IEEE Transactions on Services Computing*, 2025.

Lu, Q. Operational analysis of openai services using self-reported outages and incidents. Master’s thesis, Universiteit van Amsterdam, 2024. Available at https://atlarge-research.com/pdfs/qlu_2024.pdf.

Luo, T., Ng, K. K., Khor, Z. P., Sankhe, S., Loo, B. T., and Liu, V. Multiplexed heterogeneous llm serving via stage-aligned parallelism. In *Proceedings of the 2025 ACM Symposium on Cloud Computing*, pp. 735–747, 2025.

Ma, R., Yang, X., Wang, J., Qi, Q., Sun, H., Wang, J., Zhuang, Z., and Liao, J. Hpipe: Large language model pipeline parallelism for long context on heterogeneous cost-effective devices. In *Proceedings of the 2024 Conference of the North American Chapter of the Association for Computational Linguistics: Human Language Technologies (Volume 6: Industry Track)*, pp. 1–9, 2024.

Meta. Meta-llama/llama-3.1-8b-instruct · hugging face, Jul 2024. URL <https://huggingface.co/meta-llama/Llama-3.1-8B-Instruct>.

Miao, X., Shi, C., Duan, J., Xi, X., Lin, D., Cui, B., and Jia, Z. SpotServe: Serving Generative Large Language Models on Preemptible Instances. In *Proceedings of the 29th ACM International Conference on Architectural Support for Programming Languages and Operating Systems, Volume 2*, volume 2 of *ASPLOS ’24*, pp. 1112–1127, New York, NY, USA, April 2024. Association for Computing Machinery. ISBN 979-8-4007-0385-0. doi: 10.1145/3620665.3640411. URL <https://dl.acm.org/doi/10.1145/3620665.3640411>.

mixen56. Freeze or error using function mpi_comm_connect · issue #13076 · open-mpi/ompi, Feb 2025. URL <https://github.com/open-mpi/ompi/issues/13076>.

MPIForum. Mpi: A message-passing interface standard, 1994.

Narayanan, D., Shoeybi, M., Casper, J., LeGresley, P., Patwary, M., Korthikanti, V., Vainbrand, D., Kashinkunti, P., Bernauer, J., Catanzaro, B., et al. Efficient large-scale language model training on gpu clusters using megatron-lm. In *Proceedings of the international conference for high performance computing, networking, storage and analysis*, pp. 1–15, 2021.

Nvidia. Tensorrt llm. URL <https://github.com/NVIDIA/A/TensorRT-LLM>.

NVidia. 4.1. unified memory, Dec 2025. URL <https://docs.nvidia.com/cuda/cuda-programming-guide/04-special-topics/unified-memory.html>.

Papaioannou, K. and Doudali, T. D. The importance of workload choice in evaluating llm inference systems. In *Proceedings of the 4th Workshop on Machine Learning and Systems*, pp. 39–46, 2024.

Patke, A., Reddy, D., Jha, S., Qiu, H., Pinto, C., Narayanaswami, C., Kalbarczyk, Z., and Iyer, R. Queue management for slo-oriented large language model serving. In *Proceedings of the 2024 ACM Symposium on Cloud Computing*, pp. 18–35, 2024.

Patke, A., Reddy, D., Jha, S., Narayanaswami, C., Kalbarczyk, Z., and Iyer, R. Hierarchical autoscaling for large language model serving with chiron. *arXiv preprint arXiv:2501.08090*, 2025.

Schulz, M. The state of mpi current standard and future plans, Dec 2023. URL <https://plasma-pepsc.eu/wp-content/uploads/2024/02/2023-12-plasma-a-stateofmpi.pdf>.

ShareGPT. Sharegpt90k · datasets at hugging face. URL <https://huggingface.co/datasets/liyucheng/ShareGPT90K>.

Shoeybi, M., Patwary, M., Puri, R., LeGresley, P., Casper, J., and Catanzaro, B. Megatron-lm: Training multi-billion parameter language models using model parallelism. *arXiv preprint arXiv:1909.08053*, 2019.

Song, M., Tang, X., Hou, F., Li, J., Wei, W., Ma, Y., Xiao, R., Si, H., Jiang, D., Yin, S., et al. Xy-serve: End-to-end versatile production serving for dynamic llm workloads. In *Proceedings of the 31st ACM International Conference on Architectural Support for Programming Languages and Operating Systems, Volume 1*, pp. 314–329, 2026.

Strati, F., McAllister, S., Phanishayee, A., Tarnawski, J., and Klimovic, A. Déjàvu: Kv-cache streaming for fast, fault-tolerant generative llm serving. In *Proceedings of the 41st International Conference on Machine Learning*, pp. 46745–46771, 2024.

Sun, B., Huang, Z., Zhao, H., Xiao, W., Zhang, X., Li, Y., and Lin, W. Llumnix: Dynamic scheduling for large language model serving. In *Proceedings of the 18th USENIX Conference on Operating Systems Design and Implementation*, OSDI’24, pp. 173–191, USA, July 2024. USENIX Association. ISBN 978-1-939133-40-3.

Tiwari, D., Gupta, S., Rogers, J., Maxwell, D., Rech, P., Vazhkudai, S., Oliveira, D., Londo, D., DeBardeleben, N., Navaux, P., et al. Understanding gpu errors on large-scale hpc systems and the implications for system design and operation. In *2015 IEEE 21st International Symposium on High Performance Computer Architecture (HPCA)*, pp. 331–342. IEEE, 2015.

Wang, W., Yu, N., Xiong, S., and Liu, Z. Reliable and resilient collective communication library for llm training and serving. *arXiv preprint arXiv:2512.25059*, 2025a.

Wang, Y., Chen, Y., Li, Z., Kang, X., Fang, Y., Zhou, Y., Zheng, Y., Tang, Z., He, X., Guo, R., et al. Burstgpt: A real-world workload dataset to optimize llm serving systems. In *Proceedings of the 31st ACM SIGKDD Conference on Knowledge Discovery and Data Mining V. 2*, pp. 5831–5841, 2025b.

Wang, Z., Jia, Z., Zheng, S., Zhang, Z., Fu, X., Ng, T. S. E., and Wang, Y. GEMINI: Fast Failure Recovery in Distributed Training with In-Memory Checkpoints. In *Proceedings of the 29th Symposium on Operating Systems Principles*, SOSP ’23, pp. 364–381, New York, NY, USA, October 2023. Association for Computing Machinery. ISBN 979-8-4007-0229-7. doi: 10.1145/3600006.3613145. URL <https://dl.acm.org/doi/10.1145/360006.3613145>.

Weingram, A., Li, Y., Qi, H., Ng, D., Dai, L., and Lu, X. xcl: A survey of industry-led collective communication libraries for deep learning. *Journal of Computer Science and Technology*, 38(1):166–195, 2023.

Wu, B., Zhu, R., Zhang, Z., Sun, P., Liu, X., and Jin, X. dlora: Dynamically orchestrating requests and adapters for lorallm serving. In *18th USENIX Symposium on Operating Systems Design and Implementation (OSDI 24)*, pp. 911–927, 2024.

Xiang, Y., Li, X., Qian, K., Yang, Y., Zhu, D., Yu, W., Zhai, E., Liu, X., Jin, X., and Zhou, J. Aegaeon: Effective gpu pooling for concurrent llm serving on the market. In *Proceedings of the ACM SIGOPS 31st Symposium on Operating Systems Principles*, pp. 1030–1045, 2025.

Xu, W., Chen, C., Xiao, H., Li, K., Xiong, J., Zhang, C., Zhou, W., Tao, C., Bai, Y., Yu, B., et al. Anchortp: Resilient llm inference with state-preserving elastic tensor parallelism. *arXiv preprint arXiv:2511.11617*, 2025.

Zhang, D., Wang, H., Liu, Y., Wei, X., Shan, Y., Chen, R., and Chen, H. *blitzscale*: Fast and live large model autoscaling with $O(1)$ host caching. In *19th USENIX Symposium on Operating Systems Design and Implementation (OSDI 25)*, pp. 275–293, 2025a.

Zhang, H., Wei, T., Zheng, Z., Du, J., Chen, Z., and Lu, Y. Td-pipe: Temporally-disaggregated pipeline parallelism architecture for high-throughput llm inference. In *Proceedings of the 54th International Conference on Parallel Processing*, pp. 689–698, 2025b.

Zhao, Y. and Wang, J. Alise: Accelerating large language model serving with speculative scheduling. In *Proceedings of the 43rd IEEE/ACM International Conference on Computer-Aided Design*, pp. 1–9, 2024.

Zhong, Y., Liu, S., Chen, J., Hu, J., Zhu, Y., Liu, X., Jin, X., and Zhang, H. *distserve*: Disaggregating prefill and decoding for goodput-optimized large language model serving. In *18th USENIX Symposium on Operating Systems Design and Implementation (OSDI 24)*, pp. 193–210, 2024.

A. Additional Results

Table 1. Comparison of KEVLARFLOW and baseline under three node failure scenarios. “Base.” indicates the standard fault behavior. “Imp.” means the improvement of KEVLARFLOW over the standard fault behavior. Improvement less than 1x is caused by non-determinism in execution.

Scene	RPS	Latency Avg (s)			TTFT Avg (s)			Latency P99 (s)			TTFT P99 (s)		
		Base.	Ours	Imp.	Base.	Ours	Imp.	Base.	Ours	Imp.	Base.	Ours	Imp.
Scene 1	1.0	67.70	64.06	1.06x	0.20	0.20	1.02x	148.87	143.05	1.04x	0.33	0.34	0.97x
	2.0	146.15	67.07	2.18x	73.84	0.19	378.91x	308.48	145.92	2.11x	181.18	0.32	574.56x
	3.0	230.02	88.69	2.59x	158.11	17.30	9.14x	502.54	189.97	2.65x	391.10	61.98	6.31x
	4.0	369.08	143.29	2.58x	297.26	71.08	4.18x	789.27	326.14	2.42x	687.86	216.26	3.18x
	5.0	495.64	210.39	2.36x	422.62	140.47	3.01x	1039.56	499.11	2.08x	948.84	400.99	2.37x
	6.0	661.22	258.00	2.56x	590.29	188.27	3.14x	1366.77	613.55	2.23x	1267.99	515.41	2.46x
	7.0	867.55	349.84	2.48x	796.53	280.19	2.84x	1826.76	847.07	2.16x	1737.31	745.76	2.33x
	8.0	1074.00	449.96	2.39x	1003.40	379.47	2.64x	2252.86	1093.81	2.06x	2167.29	1003.85	2.16x
Scene 2	1.0	62.56	59.80	1.05x	0.19	0.20	0.95x	139.63	137.19	1.02x	0.33	0.34	0.96x
	2.0	65.99	65.64	1.01x	0.20	0.20	1.01x	146.18	142.87	1.02x	0.34	0.32	1.06x
	3.0	69.84	68.75	1.02x	0.20	0.20	0.99x	150.13	150.40	1.00x	0.34	0.35	0.98x
	4.0	70.85	68.22	1.04x	0.74	0.20	3.64x	152.32	148.09	1.03x	6.35	0.34	18.85x
	5.0	96.31	71.27	1.35x	25.24	1.17	21.58x	208.28	155.03	1.34x	80.55	9.84	8.18x
	6.0	140.33	88.15	1.59x	69.49	17.42	3.99x	284.19	199.84	1.42x	165.26	60.92	2.71x
	7.0	182.84	114.71	1.59x	111.47	44.10	2.53x	393.03	249.74	1.57x	285.59	123.26	2.32x
	8.0	218.79	142.49	1.54x	147.06	71.83	2.05x	475.71	303.05	1.57x	372.80	190.82	1.95x
	9.0	270.33	172.37	1.57x	198.74	101.80	1.95x	551.31	377.61	1.46x	447.16	274.88	1.63x
	10.0	308.39	212.22	1.45x	237.64	140.78	1.69x	635.05	448.57	1.42x	536.55	343.79	1.56x
	11.0	355.24	253.80	1.40x	284.79	184.06	1.55x	714.06	542.99	1.32x	615.45	448.20	1.37x
	12.0	434.45	277.38	1.57x	363.37	207.60	1.75x	887.34	585.88	1.51x	783.54	488.21	1.60x
	13.0	477.47	324.02	1.47x	405.76	253.63	1.60x	973.63	697.05	1.40x	880.20	600.52	1.47x
	14.0	557.11	385.81	1.44x	484.94	315.64	1.54x	1140.89	864.77	1.32x	1041.62	778.17	1.34x
	15.0	650.51	422.08	1.54x	578.53	351.99	1.64x	1318.74	902.43	1.46x	1223.75	803.75	1.52x
	16.0	706.36	474.50	1.49x	634.31	404.00	1.57x	1464.48	1043.13	1.40x	1371.26	966.13	1.42x
Scene 3	1.0	63.05	57.71	1.09x	0.19	0.20	0.95x	143.49	143.22	1.00x	0.32	0.70	0.45x
	2.0	69.96	64.81	1.08x	0.20	0.19	1.03x	150.65	150.89	1.00x	0.31	0.32	0.98x
	3.0	81.06	68.72	1.18x	8.96	0.20	44.96x	174.10	155.77	1.12x	47.22	0.34	139.02x
	4.0	130.50	68.85	1.90x	58.77	0.20	291.69x	279.86	158.76	1.76x	163.65	0.34	479.81x
	5.0	199.43	69.81	2.86x	127.32	0.37	344.57x	428.10	156.81	2.73x	316.37	4.29	73.78x
	6.0	242.23	85.48	2.83x	170.63	14.62	11.67x	507.31	202.63	2.50x	413.60	73.28	5.64x
	7.0	311.04	99.58	3.12x	239.55	28.56	8.39x	654.54	229.75	2.85x	545.80	104.22	5.24x
	8.0	385.38	144.88	2.66x	312.91	74.90	4.18x	823.90	338.17	2.44x	714.20	224.51	3.18x
	9.0	437.31	149.21	2.93x	365.36	78.87	4.63x	933.25	375.25	2.49x	824.20	269.82	3.05x
	10.0	499.20	194.55	2.57x	428.11	122.95	3.48x	1055.12	484.69	2.18x	960.63	380.62	2.52x
	11.0	570.28	227.11	2.51x	498.81	157.68	3.16x	1194.28	574.55	2.08x	1097.18	488.82	2.24x
	12.0	696.55	251.62	2.77x	624.73	181.55	3.44x	1466.06	634.68	2.31x	1380.21	543.45	2.54x
	13.0	743.44	295.53	2.52x	671.54	225.13	2.98x	1576.58	728.12	2.17x	1486.42	636.20	2.34x
	14.0	849.89	340.96	2.49x	778.40	271.00	2.87x	1808.74	849.81	2.13x	1725.38	769.93	2.24x
	15.0	978.17	385.28	2.54x	906.51	315.31	2.87x	2056.54	951.79	2.16x	1972.35	871.37	2.26x
	16.0	1040.73	416.90	2.50x	968.50	346.72	2.79x	2208.27	1050.98	2.10x	2137.44	971.49	2.20x